Article

A Theoretical Study of the NMR Spin–Spin Coupling Constants of the Complexes [(NC)Pt–Tl(CN)] (n = 0–3) and [(NC)Pt–Tl–Pt(CN)]: A Lesson on Environmental Effects

Jochen Autschbach, and Boris Le Guennic

J. Am. Chem. Soc., **2003**, 125 (44), 13585-13593• DOI: 10.1021/ja0368047 • Publication Date (Web): 03 October 2003

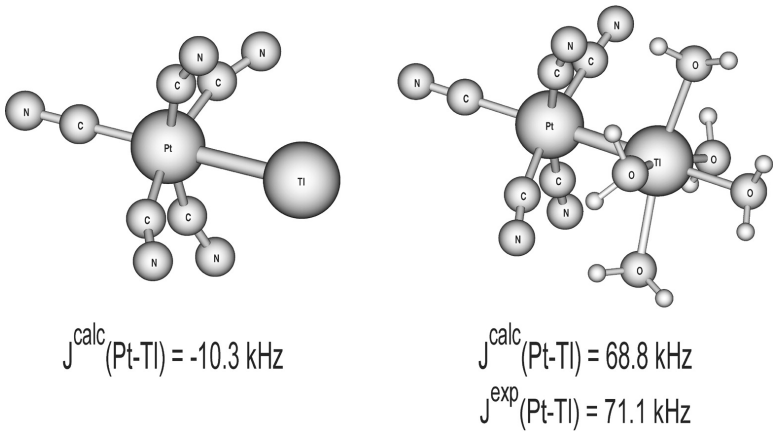

$J^{calc}(Pt\text{-}Tl) = -10.3$ kHz

$J^{calc}(Pt\text{-}Tl) = 68.8$ kHz

$J^{exp}(Pt\text{-}Tl) = 71.1$ kHz

More About This Article

Additional resources and features associated with this article are available within the HTML version:

- Supporting Information
- Links to the 4 articles that cite this article, as of the time of this article download
- Access to high resolution figures
- Links to articles and content related to this article
- Copyright permission to reproduce figures and/or text from this article

View the Full Text HTML

J|A|C|S
ARTICLES
Published on Web 10/03/2003

A Theoretical Study of the NMR Spin−Spin Coupling Constants of the Complexes $[(NC)_5Pt-Tl(CN)_n]^{n-}$ ($n = 0-3$) and $[(NC)_5Pt-Tl-Pt(CN)_5]^{3-}$: A Lesson on Environmental Effects

Jochen Autschbach*,† and Boris Le Guennic

Contribution from the Lehrstuhl für Theoretische Chemie, Universität Erlangen, Egerlandstrasse 3, D-91058 Erlangen, Germany

Received June 20, 2003; E-mail: jochena@buffalo.edu

Abstract: The molecular geometries and the nuclear spin−spin coupling constants of the complexes $[(NC)_5Pt-Tl(CN)_n]^{n-}$, $n = 0-3$, and the related system $[(NC)_5Pt-Tl-Pt(CN)_5]^{3-}$ are studied. These complexes have received considerable interest since the first characterization of the $n = 1$ system by Glaser and co-workers in 1995 [*J. Am. Chem. Soc.* **1995**, *117*, 7550−7551]. For instance, these systems exhibit outstanding NMR properties, such as extremely large Pt−Tl spin−spin coupling constants. For the present work, all nuclear spin−spin coupling constants J_{Pt-Tl}, J_{Pt-C}, and J_{Tl-C} have been computed by means of a two-component relativistic density functional approach. It is demonstrated by the application of increasingly accurate computational models that both the huge J_{Pt-Tl} for the complex $(NC)_5Pt-Tl$ and the whole experimental trend among the series are entirely due to solvent effects. An approximate inclusion of the bulk solvent effects by means of a continuum model, in addition to the direct coordination, proves to be crucial. Similarly drastic effects are reported for the coupling constants between the heavy atoms and the carbon nuclei. A computational model employing the statistical average of orbital-dependent model potentials (SAOP) in addition to the solvent effects allows to accurately reproduce the experimental coupling constants within reasonable limits.

1. Introduction

The complexes $[(NC)_5Pt-Tl(CN)_n]^{n-}$, $n = 0-3$, (**I**, **II**, **III**, and **IV**) and the related system $[(NC)_5Pt-Tl-Pt(CN)_5]^{3-}$ (**V**) have received considerable interest in experimental as well as theoretical studies. Complex **II** was first characterized by Glaser et al. in 1995.[1] Subsequently, a detailed experimental study of the whole series of complexes has been published.[2] Since then, the number of members of this class of compounds has been further extended; see, for example, refs 3 and 4. These complexes exhibit outstanding, sometimes unintuitive, NMR properties. One typical feature of the NMR spectra of complexes **I**−**V** and related compounds is the very large Pt−Tl spin−spin coupling constant (the largest coupling constants so far observed between two different nuclei).[2−4] For example, for complex **I**, the Pt−Tl coupling constant has experimentally been found to be about 71 kHz. Along the series **I** to **IV**, J_{Pt-Tl} decreases from 71 to 39 kHz (25 kHz for complex **V**).

Computational studies on complexes **I**−**IV** have so far been carried out by Pyykkö and Patzschke[5,6] (model complexes in which the CN^- groups were replaced by H^-, and the cyano complexes) and by Russo and Kaltsoyannis.[7] Reference 5 has focused on an investigation of the properties of the unusually short Pt−Tl bonds and the delocalization of these systems (see also ref 8[8]). A subsequent theoretical investigation of the cyano complexes instead of the hydride models by the same authors has a similar scope and conclusions.[6] Reference 7 has aimed at computationally reproducing the vibrational spectra and given further support for the correctness of the proposed strucures (Figure 1). Autschbach and Ziegler have previously studied the spin−spin coupling constants for complex **II**.[8] They found that effects from Tl coordination by the solvent (H_2O) could be responsible for almost half of the huge 57 kHz magnitude (exptl value) of the Pt−Tl coupling constant. However, in these computations, a difference of approximately 20% remained between the calculated and the experimental data. Because the focus of this previous paper, ref 8, has been on the unintuitive pattern of the Tl−C coupling constants (which is also due to solvent coordination), this issue was not further investigated. Also, more important for the present study, no attempt has so far been made to computationally reproduce the even larger Pt−Tl coupling constant for complex **I** and the experimentally observed decrease of J_{Pt-Tl} along the series **I**−**IV**.

† New address: Department of Chemistry, University at Buffalo, 312 Natural Sciences Complex, Buffalo, NY 14260-3000, USA.

(1) Berg, K. E.; Glaser, J.; Read, M. C.; Tóth, I. *J. Am. Chem. Soc.* **1995**, *117*, 7550−7751.
(2) Maliarik, M.; Berg, K.; Glaser, J.; Sandström, M.; Tóth, I. *Inorg. Chem.* **1998**, *37*, 2910−2919.
(3) Ma, G.; Kritikos, M.; Glaser, J. *Eur. J. Inorg. Chem.* **2001**, 1311−1319.
(4) Ma, G.; Fischer, A.; Glaser, J. *Eur. J. Inorg. Chem.* **2002**, 1307−1314.
(5) Pyykkö, P.; Patzschke, M. *Faraday Discuss.* **2003**, *124*, 41−45.
(6) Patzschke, M.; Pyykkö, P. *Inorg. Chem.*, submitted.
(7) Russo, M. R.; Kaltsoyannis, N. *Inorg. Chim. Acta* **2001**, *312*, 221−225.
(8) Autschbach, J.; Ziegler, T. *J. Am. Chem. Soc.* **2001**, *123*, 5320−5324.

10.1021/ja0368047 CCC: $25.00

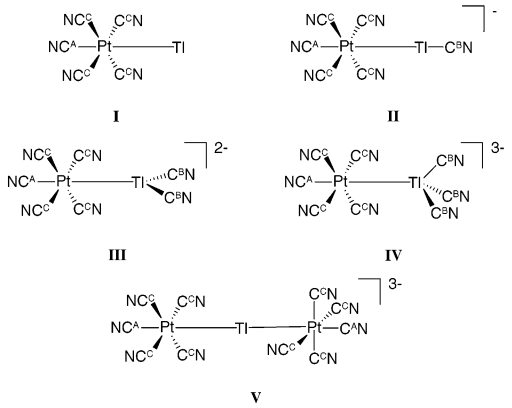

Figure 1. Proposed (see ref 2) structures for the complexes **I**−**V**. These structures were used as starting points in the geometry optimizations.

It is the purpose of the present work to demonstrate by the application of increasingly accurate computational models that both the huge J_{Pt-Tl} for complex **I** as well as the whole experimental trend is entirely due to the presence of solvent molecules (H_2O) in the NMR measurements. Without solvent, the trend would be opposite for the series **I**−**IV**, with **IV** having the largest Pt−Tl coupling constant. In this respect, an approximate inclusion of the bulk solvent effects, in addition to the directly coordinated explicit first solvation shell, proves to be crucial to inverse the trend for the free complexes to the one observed in the experiments. Similarly drastic effects are found for the coupling constants between Tl and the carbon nuclei. On the other hand, the J_{Pt-C} are somewhat less affected, though the agreement with experimental values is also significantly improved by applying a more realistic computational model. From the results obtained by our computations, and from the good agreement with experiment for our most realistic computational model, we conclude that great care must be taken when analyzing solution NMR spectra of transition metal complexes since the observed trends might be caused by environmental effects. As in other metal−metal bonded systems (see refs 9 and 10) relativistic effects serve as a "magnifying glass" for a study of changes of the metal−metal bond along a series of related complexes.

In section 2, we outline the computational details. In section 3, the results of the calculations are discussed and compared to experiment. The findings are summarized in section 4.

2. Computational Details

Density functional theory (DFT) computations have been carried out with the Amsterdam density functional (ADF) program package.[11−13] The computations employed a modified version of the code for the two-component relativistic computation of indirect nuclear spin−spin coupling constants that has been described in refs 14 and 15. It is based on the zeroth-order regular approximation (ZORA) Hamiltonian.[16,17] Recently, the performance of the program has been improved by implementing a convergence acceleration for spin−orbit calculations and by parallelizing the code.[18] In the single-point DFT calculations that preceded the determination of the spin−spin coupling constants, as well as in the spin−spin coupling calculations themselves, the self-consistent molecular Kohn−Sham potential V has been used to build the ZORA operators for reasons of consistency with a previous investigation of complex **II**.[8] It enters the kinetic energy operator and the perturbation operators via a term $\mathscr{K} = 2c^2/(2c^2 - V)$.[14] This ZORA-specific term yields $\mathscr{K} = 1$ in the nonrelativistic limit ($c \rightarrow \infty$). Here, c is the speed of light. We note that negligible changes of the results are usually obtained when V in the function $\mathscr{K}$ is chosen as a sum-over-atomic-potentials model potential instead. The latter has been employed in the geometry optimizations.[19]

The spin−spin coupling constant within the relativistic ZORA formalism consists of four terms that we denote by Fermi-contact (FC), spin-dipole (SD), and the paramagnetic and diamagnetic orbital terms (OP and OD). As in previous work,[8−10,20] we have chosen the well-known nonrelativistic nomenclature[21,22] for the four terms because, first, they yield the respective FC, SD, OP, and OD terms of Ramsey's nonrelativistic theory in the nonrelativistic limit ($c \rightarrow \infty$) and, second, they can be interpreted in a similar way.[14,23] Values for spin−spin coupling constants refer to ^{205}Tl, ^{195}Pt, and ^{13}C. If not stated otherwise, we have omitted the expensive computation of the often very small SD contribution. However, it is included in the spin−spin couplings based on spin−orbit coupled two component orbitals since its inclusion in these calculations leads only to a marginal increase in computational time. The spin−orbit contributions are not negligible but also not very large compared to the solvent effects and can thus be neglected for our samples at the present level of accuracy.

The Vosko−Wilk−Nusair (VWN) local density approximation (LDA)[24] has been used in most computations. It provides a reasonable accuracy for structures and spin−spin couplings of heavy metal complexes.[8−10,20,25] The frozen core Slater-type basis sets used for the geometry optimizations include 4f, 5spd and 6s, or 6sp as valence shells for Pt and for Tl, respectively. The 1s shell has been kept frozen for C, N, and O. All electron Slater-type basis sets, augmented with steep 1s and 2p functions in the case of Pt and Tl, have been used for the computations of spin−spin couplings as described in refs 14 and 15. All basis sets are of triple-ζ quality augmented with two polarization functions in the metal's valence shells, one polarization function for C, N, and O and are of double-ζ quality for the core shells in the case of all-electron computations.

Solvent effects have been taken into account by using two different approaches. In previous work, it was demonstrated that the sign and magnitude of the coupling constants of complex **II** and other heavy transition metal complexes can be very strongly influenced by the surrounding solvent molecules.[8,20] Therefore, in the present work, the first solvation shell is represented by explicit water molecules surrounding the Tl atom. We have further used the COSMO (COnductor-like Screening MOdel),[26−28] as implemented in ADF,[29] in order to implicitly treat the remaining bulk of the solvent as a polarizable

(9) Autschbach, J.; Igna, C. D.; Ziegler, T. *J. Am. Chem. Soc.* **2003**, *125*, 1028−1032.
(10) Autschbach, J.; Igna, C. D.; Ziegler, T. *J. Am. Chem. Soc.* **2003**, *125*, 4937−4942.
(11) Fonseca Guerra, C.; Visser, O.; Snijders, J. G.; te Velde, G.; Baerends, E. J. Parallelisation of the Amsterdam Density Functional program Program. In *Methods and Techniques for Computational Chemistry*; STEF: Cagliari, 1995.
(12) te Velde, G.; Bickelhaupt, F. M.; Baerends, E. J.; van Gisbergen, S. J. A.; Fonseca Guerra, C.; Snijders, J. G.; Ziegler, T. *J. Comput. Chem.* **2001**, *22*, 931−967.
(13) *Amsterdam Density Functional program*; Theoretical Chemistry, Vrije Universiteit: Amsterdam (URL: http://www.scm.com).
(14) Autschbach, J.; Ziegler, T. *J. Chem. Phys.* **2000**, *113*, 936−947.
(15) Autschbach, J.; Ziegler, T. *J. Chem. Phys.* **2000**, *113*, 9410−9418.
(16) van Lenthe, E.; Baerends, E. J.; Snijders, J. G. *J. Chem. Phys.* **1993**, *99*, 4597−4610.
(17) Dyall, K.; van Lenthe, E. *J. Chem. Phys.* **1999**, *111*, 1366−1372.
(18) Autschbach, J. Unpublished.
(19) van Lenthe, E.; Ehlers, A.; Baerends, E. J. *J. Chem. Phys.* **1999**, *110*, 8943−8953.
(20) Autschbach, J.; Ziegler, T. *J. Am. Chem. Soc.* **2001**, *123*, 3341−3349.
(21) Ramsey, N. F. *Phys. Rev.* **1953**, *91*, 303−307.
(22) Pyykkö, P. *Theor. Chem. Acc.* **2000**, *103*, 214−216.
(23) Wolff, S. K.; Ziegler, T.; van Lenthe, E.; Baerends, E. J. *J. Chem. Phys.* **1999**, *110*, 7689−7698.
(24) Vosko, S. H.; Wilk, L.; Nusair, M. *Can. J. Phys.* **1980**, *58*, 1200−1211.
(25) Autschbach, J.; Ziegler, T. Relativistic Computation of NMR Shieldings and Spin−spin Coupling Constants. In *Encyclopedia of Nuclear Magnetic Resonance*; Grant, D. M., Harris, R. K., Eds.; John Wiley & Sons: Chichester, 2002; Vol. 9.
(26) Klamt, A.; Schüürmann, G. *J. Chem. Soc., Perkin Trans. 2* **1993**, 799−805.

continuum.[30,31] (The radii of the atomic spheres used in the COSMO calculations are 1.39, 1.7, 2.2, 1.4, 1.3, and 1.16 Å for Pt, Tl, C, N, O, and H, respectively. The metal radii are not optimized. However, in the studied complexes, the metal atoms are not in a direct contact with the solvent surface. A modification of the metal radii should not change the computational results by a significant amount.) It has previously been demonstrated that usually the innermost solvent shell has to be included explicitly[32] when computed nuclear shieldings are to be directly compared to experimental data. The same can be expected for spin−spin coupling constants. See, for example, ref 20.

No specific program development was necessary in order to use the ADF COSMO implementation in conjunction with the spin−spin coupling code. The reason for this lies in the fact that in the calculation of the spin−spin coupling constants the perturbations due to the nuclear spins cause no change of the electron density. It is the latter, however, that is responsible for the self-consistently determined COSMO surface charges. The electrostatic potential of these charges in turn enters the molecular Kohn−Sham equations.[29] The most important FC (and also the SD) spin−spin coupling mechanism causes mainly a change of the molecule's electronic spin-density, thus there is no perturbation of the COSMO part of the Kohn−Sham potential. The same is true for the OP mechanism which causes mainly a perturbation of the current density. We note that the latter is not treated self-consistently in our approach since we use an "uncoupled" nonhybrid DFT formalism in which the current density is not considered in the energy functional. The spin-density perturbation is presently approximated by the first-order perturbed VWN potential.[14,33] When electronic spin−orbit coupling is considered there is in addition a perturbation of the current density by the FC/SD mechanism, and of the spin-density by the OP mechanism (FC/SD − OP spin−orbit cross terms). The electron density, and thus the COSMO part of the Kohn−Sham potential, remains unaltered. In the case when a hybrid density functional such as B3LYP[34] is employed, a "coupled" procedure as recently outlined in ref 35 must be adopted. In our case, the only contribution of the COSMO potential in the spin−spin coupling code would be in the ZORA perturbation operators, viz. in the potential V that enters the function $\mathscr{K}$ which has been mentioned above. This effect must be expected to be negligible for the same reason that the (supposedly larger) difference between a model potential and the full Kohn−Sham potential in $\mathscr{K}$ does not yield a noticeable difference in the results. The COSMO portion of V has thus not been used in the present study to build the perturbation operators.

The "statistical average of orbital-dependent model potentials" (SAOP) Kohn−Sham potential has been previously designed for and successfully applied to excitation energies and frequency dependent response properties.[36−40] Poater et al. have recently reported that SAOP results show considerable improvement with respect to other potentials, such as VWN or Becke−Perdew (BP),[41,42] for a range of NMR chemical shifts.[43] In the present work, we have investigated its impact on the calculation of spin−spin coupling constants.

Table 1. Selected Calculated Bond Lengths (in angstrom) for Complexes **I**−**V**

	R(Tl–Pt)	R(Tl–C^B)	R(Pt–C^A)	R(Pt–C^C)	R(Tl–O)[e]
		complex **I**			
unsolvated[a]	2.874		1.912	1.979	
model A (3 H_2O)[b]	2.687		1.952	1.991	2.415
model A (4 H_2O)	2.641		1.965	1.989	2.451
model A (5 H_2O)	2.630		1.982	1.989	2.492
model B[c]	2.630		2.011	1.988	2.380
exptl[d]	2.627(2)		2.003(1)		
		complex **II**			
unsolvated	2.578	2.178	1.957	1.999	
model A (4 H_2O)	2.653	2.174	2.005	1.985	2.540
model B	2.659	2.180	2.019	1.984	2.486
exptl	2.598(3)	2.128(6)	2.009(2)		2.505(5)
		complex **III**			
unsolvated	2.617	2.238	1.995	2.002	
model A (2 H_2O)	2.649	2.241	2.013	1.992	2.601
model B	2.646	2.201	2.027	1.986	2.492
exptl	2.618(4)	2.206(2)	2.003(2)		
		complex **IV**			
unsolvated	2.689	2.277	2.034	2.001	
model B	2.659	2.225	2.034	1.990	
exptl	2.638(4)	2.203(6)	2.008(2)		
		complex **V**			
unsolvated	2.663		2.025	2.001	
model A (4 H_2O)	2.709		2.050	1.989	2.686
model B	2.668		2.042	1.983	2.636
exptl					

[a] Scalar relativistically optimized geometry, no solvent, LDA functional. [b] Model A: scalar relativistically optimized geometry including explicit first solvation shell, LDA functional. [c] Model B: model A + COSMO for the bulk solvent effects. [d] Reference 44. [e] Average distance.

Results and Discussion

3.1. Geometries. The computed molecular geometries for the compounds **I**−**V** are listed in Table 1. The symmetry of the unsolvated molecules was taken as C_{4v}, C_{4v}, C_{2v}, C_s, and D_{4d} for $[(NC)_5Pt–Tl(CN)_n]^{n-}$ ($n = 0–3$) and $[(NC)_5Pt–Tl–Pt(CN)_5]^{3-}$, respectively. In a recent study using several levels of approximation including HF, MP2, and B3LYP, Pyykkö and Patzschke have investigated the properties of the Pt−Tl bond in simplified hydride models for the complexes **I**−**III** (the CN^- groups have been replaced by H^-).[5] By comparison of the geometries obtained with the different methods, it has been shown that spin−orbit effects are not very important, whereas scalar relativistic effects have a large impact on the geometry of these systems. For the different models, the BP functional yielded Pt−Tl distances shorter than the experimental values. However, this comparison has to be carefully done because the change of the ligands from CN^- to H^- will significantly affect the geometry. By using a Pauli quasi-relativistic method, Russo and Kaltsoyannis have previously obtained very good agreement with the experimental data for complexes **II**−**IV**, but calculations strongly overestimated the Pt−Tl bond length for the complex **I**.[7] It is known that the BP functional tends to yield somewhat too long bond distances. Even with the use of the ZORA formalism without the BP functional for exchange and correlation, we have also obtained a much too long Pt−Tl bond (2.874 vs 2.627 Å) for the complex **I**. However, the calculated

(27) Klamt, A. *J. Phys. Chem.* **1995**, *99*, 2224−2235.
(28) Klamt, A.; Jones, V. *J. Chem. Phys.* **1996**, *105*, 9972−9981.
(29) Pye, C. C.; Ziegler, T. *Theor. Chem. Acc.* **1999**, *101*, 396−408.
(30) Cramer, C. J.; Truhlar, D. G. *Chem. Rev.* **1999**, *99*, 2161−2200.
(31) Tomasi, J.; Persico, M. *Chem. Rev.* **1994**, *94*, 2027−2094.
(32) Mennucci, B.; Martinez, J. M.; Tomasi, J. *J. Phys. Chem. A* **2001**, *105*, 7287−7296.
(33) Patchkovskii, S.; Autschbach, J.; Ziegler, T. *J. Chem. Phys.* **2001**, *115*, 26−42.
(34) Hertwig, R. H.; Koch, W. *Chem. Phys. Lett.* **1997**, *268*, 345−351.
(35) Ruud, K.; Frediani, L.; Cammi, R.; Mennucci, B. *Int. J. Mol. Sci.* **2003**, *4*, 119−134.
(36) Schipper, P. R. T.; Gritsenko, O. V.; van Gisbergen, S. J. A.; Baerends, E. J. *J. Chem. Phys.* **2000**, *112*, 1344−1352.
(37) Gritsenko, O. V.; Schipper, P. R. T.; Baerends, E. J. *Int. J. Quantum Chem.* **2000**, *76*, 407−419.
(38) Chong, D. P.; Gritsenko, O. V.; Baerends, E. J. *J. Chem. Phys.* **2002**, *116*, 1760−1772.
(39) Grüning, M.; Gritsenko, O. V.; van Gisbergen, S. J. A.; Baerends, E. J. *J. Chem. Phys.* **2002**, *116*, 9591−9601.
(40) van Gisbergen, S. J. A.; Pacheco, J. M.; Baerends, E. J. *Phys. Rev. A* **2001**, *63*, 63201.
(41) Becke, A. D. *Phys. Rev. A* **1988**, *38*, 3098−3100.
(42) Perdew, J. P. *Phys. Rev. B* **1986**, *33*, 8822−8824.
(43) Poater, J.; van Lenthe, E.; Baerends, E. J. *J. Chem. Phys.* **2003**, *118*, 8584−8593.

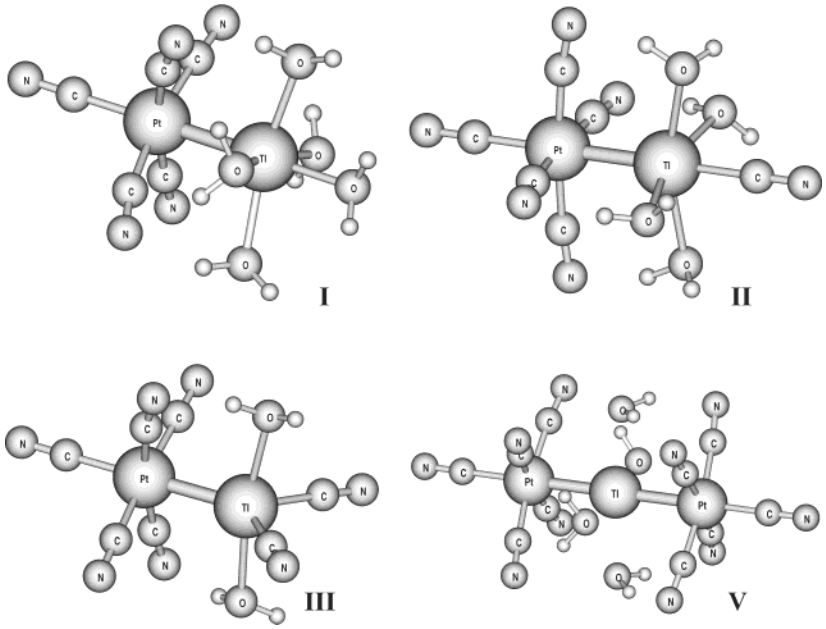

Figure 2. Scalar relativistically optimized structures of the solvated complexes **I**−**III** and **V**.

Pt−Tl distances of the other complexes compare rather well with the available experimental values of 2.578 versus 2.598 Å, 2.617 versus 2.618 Å, and 2.689 versus 2.638 Å for the complexes **II**−**IV**, respectively. Pt−C and Tl−C distances have also been well reproduced by our calculations (Table 1).

The experimental data on which our comparison is based have been obtained in aqueous solution. As suggested separately by Russo and Kaltsoyannis[7] and one of us,[8] coordination of the Tl atom by one or more water molecules will certainly occur and it may be a reason for the discrepancy between theoretical and experimental values for the complex **I**. To simulate the solvated complexes, geometry optimizations have been carried out including three, four, and five water molecules bound to the Tl atom for the complex **I** and four, two, and four water molecules for the complexes **II**, **III**, and **V** respectively. Experimental evidence for such arrangements is reported in the literature.[44] The optimized structures of solvated complexes **I**−**III** and **V** have been validated as minima on the potential energy surface by frequency calculations. Some of these optimized arrangements are shown in Figure 2. Following the suggestion made by Russo and Kaltsoyannis,[7] no first shell coordination by water molecules has been considered to occur for the complex **IV**, owing to the high number of cyanide ligands on the Tl atom and its pseudo-tetrahedral geometry. As expected, a significant shortening of the Pt−Tl bond is observed for the solvated complex **I**, and the agreement between the experimental and computed bond lengths becomes very good. To better understand the influence of the direct solvent coordination, we have considered three different environments around the Tl atom with three, four, or five water molecules, respectively. For complex **I**, it appears from the comparison of the Pt−Tl bond lengths of the optimized structures that the higher the coordination of Tl by water molecules, the shorter is the Pt−Tl distance. With five water molecules, the Pt−Tl distance is almost exactly the same as the experimental value. In the previous works by Autschbach and Ziegler[8] and Russo and Kaltsoyannis,[7] the effect of coordinated water molecules on the structural arrangement of the other studied complexes was not large. Likewise, in our present calculations, the Pt−Tl bond length increased only by about 0.08, 0.03, and 0.05 Å for the complexes **II**, **III**, and **V**, respectively, with the Pt−C and Tl−C distances also being only slightly altered.

The addition of the bulk solvent effects by using the COSMO model (model B) does not strongly affect the previously described optimized geometries of the solvated complexes **I**, **II**, and **III**. However, it should be kept in mind that spin−spin coupling constants are very sensitive toward small changes in the molecular geometries. For the complex **V**, the bulk solvent effects blur the role of the directly coordinated water molecules on the Pt−Tl bond length by a decrease of this distance which becomes similar to the one obtained for the unsolvated complex. The COSMO model affects as well the geometry of the complex **IV** with a decrease of the Pt−Tl and Tl−C^B bond lengths which are still overestimated when compared to the experimental values.

3.2. Coupling Constants. Different computational methods applied to several structural arrangements have been used in order to improve the agreement between computed and experimental indirect spin−spin coupling constants for the complexes **I**−**V**. In a previous study of complex **II**, it was demonstrated that the solvent effects, represented by water molecules coordinated to the Tl atom, shift the Pt−Tl coupling constant by more than 20 kHz toward the experimental value.[8] The relativistic increase of s-orbital density at the heavy nuclei and the charge donation by the solvent were found to be responsible for the large magnitude of J_{Pt-Tl}. In the present work, we have first applied this approach of adding an explicit solvation shell to all the studied complexes ("model A", except for complex **IV**). Recently, some studies have also demonstrated that treating the solvent implicitly as a polarizable continuum may have non-negligible contributions to the nuclear magnetic shieldings,[45−47] and also to the spin−spin coupling constants.[46−48] In the ADF code, such an approach is available in the form of the COSMO model.[29] Therefore, to take into account simulta-

(44) Jalilehvand, F.; Maliarik, M.; Sandström, M.; Mink, J.; Persson, I.; Persson, P.; Tóth, I.; Glaser, J. *Inorg. Chem.* **2001**, *40*, 3889−3899.

Table 2. Spin−Spin Coupling Constants (in hertz) for Complexes **I**−**V**[a]

	$^1J_{Tl-Pt}$	$^2J_{Tl-C}{}^A$	$^1J_{Tl-C}{}^B$	$^2J_{Tl-C}{}^C$	$^1J_{Pt-C}{}^A$	$^2J_{Pt-C}{}^B$	$^1J_{Pt-C}{}^C$
			complex **I**				
unsolvated[b]	−10262	379		−51	1555		919
	(−10352)[c]	(456)		(−19)	(1575)		(884)
model A (3 H_2O)[d]	8160	7972		−493	1367		936
model A (4 H_2O)	17930	8972		−484	1322		931
model A (5 H_2O)	24421	9895		−464	1243		945
	(20336)	(9353)		(−476)	(1244)		(926)
model B[e]	54375	11507		−298	1008		912
model C[f]	68814	14742		−313	1082		945
exptl[g]	71060	12746		592	909		820
			complex **II**				
unsolvated	14381	5524	−5855	−369	1366	116	858
	(10828)	(5219)	(−6571)	(−372)	(1382)	(88)	(839)
model A (4 H_2O)	37298	7897	2746	−306	1044	119	907
model B	47882	8761	5054	−224	929	114	911
model C	58744	10794	3753	−223	973	165	947
exptl	57020	9743	2446	452	843	200	821
			complex **III**				
unsolvated	34830	7475	−2886	−362	1116	121	864
model A (2 H_2O)	40955	8061	−900	−307	1003	105	893
model B	39780	7248	995	−211	903	103	902
model C	49294	9014	106	−190	922	130	944
exptl	47260	8446	876	338	783	128	832
			complex **IV**				
unsolvated	44921	7897	−904	−247	865	99	898
model B	35050	6414	122	−192	853	89	904
model C	43507	7929	−494	−162	857	106	949
exptl	38760	7270	52	255	742	0	843
			complex **V**				
unsolvated	5496	2376		−204	898		902
model A (4 H_2O)	25163	5128		−187	785		955
model B	26901	5274		−182	806		955
model C	29609	5751		−204	808		996
exptl	25168	4600		308	700		858

[a] Couplings refer to ^{205}Tl, ^{195}Pt, and ^{13}C. FC + PSO + DSO contribution is included in the scalar relativistic computations; SD contribution is additionally present in spin−orbit computations. [b] Scalar relativistic couplings from scalar relativistically optimized geometry, no solvent. [c] In parentheses, relativistic spin−orbit computation is based on scalar relativistic geometry. [d] Model A: complex plus specified number of explicit water molecules, geometry scalar relativistically optimized, LDA functional. [e] Model B: model A + COSMO for the bulk solvent effects. [f] Model C: model B with SAOP potential. [g] Reference 44, signs were not determined.

neously the explicit first and implicit bulk solvent effects, the "model B" consists of the reoptimized explicitly solvated molecules embedded in a polarizable continuum. This model might give a good representation of the effects of both the direct coordination of the Tl by solvent molecules and the electrostatic interaction with the bulk solvent. Third, it has recently been found that the use of the statistical average of orbital-dependent model potentials (SAOP) increases the accuracy of calculated NMR chemical shifts as compared to VWN or BP.[43] Therefore, we have applied this SAOP potential in calculations that are otherwise identical to model B. This approach is termed "model C". It should be expected from the increasingly accurate modeling of the electronic structure of the complexes and their environment that models A, B, and C yield increasing improvement of the calculated NMR properties when compared to experiment.

The experimentally observed and computed nuclear spin−spin coupling constants for complexes **I**−**V** are collected in Table 2 and graphically displayed in Figure 3. In the discussion, we will focus on the one-bond Pt−Tl coupling constants, but as shown in Figure 3, most of the conclusions can be extended to the one- and two-bond metal−carbon couplings. We have also studied the influence of electronic spin−orbit coupling on the computed couplings for some examples including a solvated complex (in parentheses in Table 2). As previously found for complex **II**,[8] the coupling constants are somewhat but not too strongly influenced by spin−orbit coupling. Therefore, this allows a discussion at the scalar relativistic level. The SD mechanism was found to be unimportant for the investigated coupling constants. The contribution to the spin−spin couplings due to the electronic orbital angular momentum (OD and OP mechanisms) are also small. All coupling constants are dominated by the Fermi-contact mechanism.

There is no qualitative agreement between the computed and experimental coupling constants for the free molecules. The experimentally observed trend is not reproduced. For complex **I**, the disagreement between the computations on the free complex and the experimental $^1J_{Pt-Tl}$ exceeds 80 kHz. Only the complex **IV** for which the coordination on the Tl atom is saturated by the CN ligands presents an acceptable agreement with the experimental $^1J_{Tl-Pt}$. The same trend is observed for the two-bond $Tl-C^A$ coupling constants. For all complexes, the $^1J_{Pt-C}{}^A$ is overestimated, whereas the $^1J_{Tl-C}{}^B$ is underestimated by the calculation on the free complexes.

(45) Cammi, R.; Mennucci, B.; Tomasi, J. *J. Chem. Phys.* **1999**, *110*, 7627−7638.
(46) Mikkelsen, K. V.; Ruud, K.; Helgaker, T. *J. Comput. Chem.* **1999**, *20*, 1281−1291.
(47) Pecul, M.; Sadlej, J. *Chem. Phys.* **1998**, *234*, 111−119.
(48) Pecul, M.; Sadlej, J. *Chem. Phys.* **2000**, *255*, 137−148.

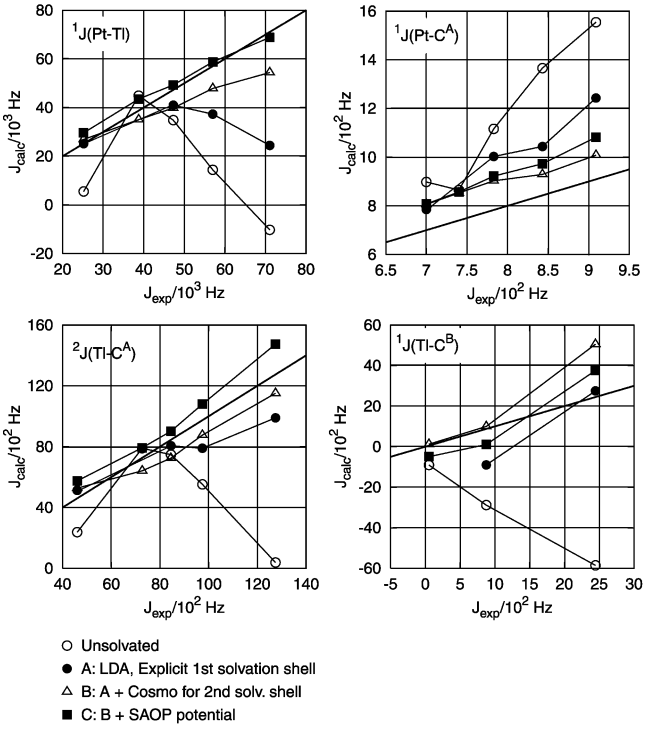

Figure 3. Comparison of density functional and experimental spin−spin coupling constants for different computational approaches. See footnotes of Table 2 for explanation of the computational models. The straight thick line indicates where $J_{calc} = J_{exp}$. The lines connecting the points do not represent fits to the data points but were added to guide the eye.

The increase of the computed Pt−Tl couplings due to the explicit inclusion of solvent molecules (model A) is remarkably large. For instance, the Pt−Tl couplings are shifted by about 30, 20, and 20 kHz for the complexes **I**, **II**, and **V** respectively. As mentioned previously,[8] this increase exceeds the solvent effects reported earlier[20] for coordinatively unsaturated Pt and Hg complexes. In this previous work, it was argued that charge donation from the solvent to the heavy metal atom and into the metal−ligand σ bonds is the dominant factor responsible for the large positive shift of the FC contribution to the coupling. We should also notice that, as expected, the higher the coordination of Tl by the cyano ligands, the smaller is the effect of the coordination of additional solvent molecules on the different coupling constants. The effect on the Pt−Tl coupling from the different numbers of solvent molecules coordinated to the Tl atom in complex **I** corroborates this conclusion, with a $^1J_{Tl-Pt}$ about 3 times higher with five than with three surrounding water molecules.

The implicit addition of the bulk solvent (model B) to the previously described model A further increases significantly the accuracy of the calculated coupling constants with respect to the experimental data. Contrary to results previously obtained for unsolvated and explicitly solvated Hg and Pt complexes,[20] the experimental trend for $^1J_{Pt-Tl}$ in the present samples is reproduced only at the level of model B. Thus qualitative agreement with experiment is observed for the different computed coupling constants (Figure 3). However, there is still a considerable difference between computed with model B and experimental Pt−Tl couplings for the lower CN-coordinated complexes. For instance, this error is about 16.7, 9.1, and 7.5 kHz for the complexes **I**, **II**, and **III**, respectively.

The calculations based on the SAOP potential (model C) give rise to another positive shift of the Pt−Tl coupling constants with respect to model B. The $^2J_{Tl-C}{}^A$ and $^1J_{Pt-C}{}^A$ are also positively shifted, whereas the $^1J_{Tl-C}{}^B$ becomes smaller: The signs of the two-bond Tl−C^C (as well as the other) coupling constants were not determined in the experiments, but the computations indicate that they are probably negative. In the recent work of Poater et al.,[43] the improvement of the chemical shift calculation due to the SAOP potential has been attributed to the increase in the gap between highest occupied and lowest vacant orbitals, thus correcting the excessively large paramagnetic contributions. In the present work, the improvement of the Pt−Tl coupling constant calculation is not governed by a strong modification of the (very small) OP term but by another substantial increase of the large FC contributions. At this stage of the discussion, it is worthwhile to point out that the model including both solvent effects and the SAOP potential (model C), allows to reproduce the experimental Pt−Tl coupling constants within 5 kHz (relative errors of 3, 3, 4, 12, and 18% for **I** to **V**, respectively). Taking the difference of more than 80, 40, and so forth kHz, for instance, in $^1J_{Tl-Pt}$ from the free complex calculations with respect to experiment into consideration, by applying model C, we have indeed come a long way toward a quantitative reproduction of the experimental data.

Our choice of models A and B is somewhat arbitrary, since the SAOP potential could also be applied for instance in the free complex or in the model A. Nevertheless, it is important to keep in mind that the (at present best) computational model C includes both solvent effects and the SAOP potential, whereas the "unsolvated" model takes into account neither the environment effects nor the SAOP potential. Only the models which include the solvent are meaningful when comparing the results with experimental *J*-couplings. Different other intermediate models could have been chosen. The description of the results obtained from all the possible combinations would have caused a large increase of data and necessary computation time, but offers little to learn in addition. An important point is that the effects which distinguish the models are not additive; that is, for instance, the application of the SAOP potential to a free complex or to a solvated one (by adding coordinated water molecules, by using the COSMO model, or by treating both of them) does not increase the Pt−Tl spin−spin coupling constant with respect to the LDA values by the same amount. This is perhaps not surprising since the asymptotically correct SAOP potential is likely to be very different from the LDA potential in the region of the van der Waals surface of the molecules (where the COSMO solvent accessible surface is constructed). As an example, the Pt−Tl spin−spin coupling constants have been computed for the complex **I** by different ways. In addition to the results given in the Table 2, the Pt−Tl coupling constant is calculated as 27195 and −9402 Hz when applying the COSMO model and the SAOP potential individually to the free complex, respectively, and 29510 Hz when the SAOP potential is applied to the model A. Generally, omitting the first explicit solvent shell and just applying the COSMO did not yield results close to the experimental Pt−Tl couplings for **I**, **II**, **III**, and **V**, regardless of whether the SAOP potential was applied or not.

3.3. Discussion. In light of the findings in the previous section, it is perhaps problematic to speak of "environmental effects on the free complexes" when they reach such magni-

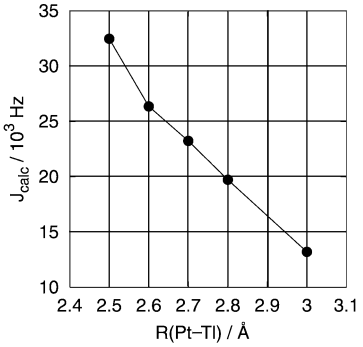

Figure 4. Dependence of the spin−spin coupling constant $^1J_{Tl-Pt}$ on the Pt−Tl distance for the solvated complex **I**. Five water molecules are coordinated to the Tl atom. The relative energies with respect to the equilibrium energy of the complexes with smaller Pt−Tl distances than R_e = 2.630 Å are 0.19 and 0.10 eV. The relative energies of the complexes with larger Pt−Tl distances are 0.66, 0.73, and 0.46 eV, respectively (from left to right).

tudes. For instance, for complex **I**, the measured coupling constant is 71 kHz, but the calculated "intrinsic" coupling constant is around −10 kHz. In this case, it might be more appropriate to think of the solvated complexes as different systems, namely their (weakly bound) aquo complexes. Even when this is taken into consideration, though, the bulk solvent effects, and the ones arising from the simultaneous application of the SAOP Kohn Sham potential instead of the VWN functional, are remarably large.

It is tempting to find a simple, intuitive explanation for the increase in the coupling constant due to the different effects: explicit coordination by water, bulk solvent effects, and the influence of the SAOP potential versus more conventional density functionals. First of all, we would like to note that from the data in Tables 1 and 2 no obvious correlation of the Pt−Tl coupling constant with the Pt−Tl bond length *R*(Pt−Tl) of the different models is visible. Whereas the Pt−Tl distance decreases in complex **I** along the series of models A, B, and C, with increasing J_{Pt-Tl}, this is not uniformly so for the other complexes. At the same time, there is indeed a very pronounced dependence of J_{Pt-Tl} on *R*(Pt−Tl), as is shown in Figure 4. The data have been obtained for complex **I** with varying fixed values of *R*(Pt−Tl) and all other geometrical variables optimized. A qualitative similar behavior is found in case the geometries are not reoptimized. For the free complex, a similarly strong dependence is observed. In the previous study of complex **II**,[8] it was also found that J_{Pt-Tl} increases with decreasing *R*(Pt−Tl). This is the reason previously, for complex **II**, that a "better", that is, larger Pt−Tl coupling constant was obtained for model A but for a geometry based on the Pauli operator. The underestimation of *R*(Pt−Tl) as compared to experiment already seemed to indicate a slight onset of a variational collapse due to the presence of the two heavy atoms. The present study confirms that the longer metal−metal bonds obtained with the variationally stable ZORA describe the systems much more realistically. It should be noted that the conclusions of ref 8 remain unaffected by these changes in the geometry of complex **II**, though, at the level of model A, quantitative agreement with the experimental J_{Pt-Tl} could not be achieved. An explanation of the large positive shift of the metal−metal and metal−ligand coupling constants has been given in terms of a small charge donation from the solvent molecules into the metal−metal and metal−ligand bonds.

Table 3. HOMO−LUMO Gaps for the Different Models and Mulliken and Hirshfeld Charge Analyses

complex	I	II	III	IV	V
HOMO−LUMO gap (eV)					
unsolvated	1.43	3.57	3.65	3.90	2.83
model A	2.76	3.82	3.79		2.88
model B	3.26	3.70	4.07	4.12	3.12
model C	3.22	3.72	3.91	3.90	2.84
Pt−Tl Mulliken overlap population (electrons)					
unsolvated	0.12	0.31	0.30	0.28	0.28
model A	0.21	0.26	0.27		0.21
model B	0.20	0.25	0.21	0.25	0.17
model C	0.19	0.23	0.19	0.23	0.14
s(Pt)−s(Tl) Mulliken overlap population (10^{-3} electrons)					
unsolvated	9.20	43.7	38.4	37.5	32.0
model A	3.90	26.5	27.2		15.7
model B	4.55	27.8	11.3	25.4	12.0
model C	15.6	29.4	8.90	22.5	18.1
s(Pt) net populations (electrons, 1s to 6s)					
unsolvated	10.4	10.4	10.4	10.4	10.4
model A	10.5	10.4	10.4		10.5
model B	10.5	10.4	10.4	10.4	10.5
model C	10.4	10.4	10.4	10.3	10.5
s(Tl) net populations (electrons, 1s to 6s)					
unsolvated	11.9	11.3	11.2	11.0	11.3
model A	11.3	11.1	11.1		11.2
model B	11.0	11.0	11.0	10.9	11.1
model C	11.0	11.0	11.0	10.9	11.1
Pt Mulliken total gross charge					
unsolvated	−0.51	−0.73	−0.75	−0.72	−0.71
model A	−0.61	−0.67	−0.72		−0.65
model B	−0.67	−0.70	−0.72	−0.71	−0.71
model C	−0.40	−0.41	−0.43	−0.41	−0.44
Tl Mulliken total gross charge					
unsolvated	0.84	0.92	0.74	0.52	0.99
model A	1.33	1.07	0.89		1.13
model B	1.57	1.21	0.91	0.58	1.31
model C	1.95	1.55	1.21	0.82	1.69
Pt Hirshfeld charge					
unsolvated	0.45	0.38	0.35	0.32	0.32
model A	0.40	0.37	0.35		0.33
model B	0.36	0.36	0.33	0.32	0.33
model C	0.38	0.37	0.34	0.33	0.34
Tl Hirshfeld charge					
unsolvated	0.70	0.60	0.42	0.28	0.43
model A	0.48	0.40	0.36		0.32
model B	0.50	0.42	0.36	0.30	0.32
model C	0.60	0.52	0.44	0.37	0.40

A criterion which is frequently used in analyses of second-order properties, to which spin−spin couplings also belong, is the gap $\Delta\epsilon$ between occupied and unoccupied MOs. As, for example, described in ref 25, the inverse of $\Delta\epsilon$ directly enters the expression of the coupling constant. Thus the smaller the energy gaps are, the larger the coupling constant might expected to be. If the HOMO−LUMO gap (HLG) is taken as a rough estimate of these trends, it can be seen from Table 3 that the trend for J_{Pt-Tl} in the free complexes does not at all follow the inverse HLG but in fact the opposite trend. The complex with the largest HLG has also the largest J_{Pt-Tl}. Such a trend has in fact already been noted for the spin−orbit contributions to the ^{13}C shielding constants in 5d transition metal carbonyls[49] which are conceptually very similar to the FC mechanism.[25] The analysis demonstrated that the increase in the HLG along the row of the periodic table was in fact outweighed by an increase

(49) Wolff, S. K.; Ziegler, T. *J. Chem. Phys.* **1998**, *109*, 895−905.

in the s-character of the metal−ligand bonds. It is thus likely that similar trends hold for the present systems, also when comparing the different computational models.

For a detailed analysis of a coupling constant, one further needs to consider the magnitude of the s-contributions in the metal−metal bond (for J_{Pt-Tl}). For this purpose, we have calculated the Mulliken overlap populations and the Mulliken net populations per s-, p-, d-, and f-type basis functions (We use the word "population" here in the usual sense, i.e., referring to the number of electrons per atom or per basis function (-type). The word "charge", also used here in its conventional meaning, indicates the charge per atom, i.e., the sum of the positive nuclear charges minus the number of electrons). On one hand, an increase in the s-to-s population between Pt and Tl would seem to indicate a larger s-character in the bond and thus a larger coupling constant. On the other hand, the detailed analysis of complex **II** in ref 8 has already shown that these complexes with their pronounced multicenter C−Pt−Tl bonds are not so easy to understand. It is just as important to consider which of the unoccupied orbitals of the free complexes, and to what extent, become partially occupied upon explicit solvation[8,20] and generally the s-character of the unoccupied antibonding MOs which do not show up in the population analysis. From Table 3, it can be seen that the Pt−Tl s-to-s overlap populations do not follow the trend for the computed J_{Pt-Tl} for the different models. At the same time, there is a trend of decreasing Tl s-net populations along the series free-complex−model A−model B−model C, along with increasing Tl gross charges. For Pt, no such trend is visible. It must be noted, though, that the application of the notoriously unreliable Mulliken charge analysis to the differently coordinated systems can be rather problematic. Thus, it is possible that the observed trends are to some extent artificial, in particular, where the coordination of the Tl differs. The Hirshfeld charges (Table 3), being derived from a *spatial* criterion rather than by assigning electrons to basis function centers, are considered to be more reliable[12] and do not at all show the trends that are present in the Mulliken charges. Though, as already mentioned, an interpretation of the Mulliken charges is problematic, we believe that something can be learned from the disagreement between the Mulliken and the Hirshfeld charges in our samples. The results suggest that there is a very strong rearrangement of electrons in particular around the Tl center taking place upon explicit solvation (model A) but also when models B and C are further applied. This rearrangement has a large impact on the s and p contributions to the Tl−Pt bonding and antibonding orbitals. From the Hirshfeld charges, it can be seen that this rearrangement must take place within the radius of the Tl atom (i.e., where the electron density of the Tl atom is high). At the same time, both metal centers become less positively (Hirshfeld) charged upon solvation of the complexes, indicating the charge donation from the solvent. We note that the oxygen Mulliken gross charges are typically 0.15 more positive in model A compared to free water (which already sums up to about 0.6 for four coordinating waters). The Mulliken charge of the O atom in free water was thereby calculated as −0.68, whereas the Hirshfeld charges are smaller in magnitude (−0.31 in free water and between −0.22 and −0.27 in model A). Apparently the charge donation is such that the Mulliken analysis still assigns a portion of the electronic density to the oxygen atoms, though it is spatially already closer to the Tl atom.

In summary, the trend in the free complexes is reminiscent of the case of Hg crown−ether complexes that has recently been investigated by Autschbach and Ziegler.[10] It was demonstrated that a hypothetical bare metal−metal fragment would have a very large coupling constant which is then reduced by (a) coordination (number of ligands and coordination strength), in particular, in trans position to the respective other metal (axial coordination) and (b) polarization of the metal−metal fragment. It can be seen that the free complex **I**, which is the most "unbalanced" of all five, has the smallest coupling constant, very similar to the previously investigated strongly polarized Hg_2^{2+}−(18-crown-6) complex of ref 10. On the other hand, the trends for the solvated complexes appear to be similar to the previously studied case of Pt−Pt coupling constants.[9] There, the coupling constants of a coordinatively saturated Pt−Pt fragment and their dependence on the σ-coordinative strength of the axial ligands were investigated. It was demonstrated that the stronger the axial ligands interact with the metal−metal fragment, the smaller the metal−metal coupling constant becomes. This situation is similar to the solvent complexes of **I** to **V** which have a different number of weakly interacting (*and* charge donating) H_2O and strongly interacting CN^- ligands. At the same time, effects on the HLG and the metal−metal distances have to be considered as well, the final result being obtained from a balance of a number of contributing factors.

4. Summary

We have calculated the spin−spin coupling constants for the heavy metal complexes $[(NC)_5Pt-Tl(CN)_n]^{n-}$, $n = 0-3$, and $[(NC)_5Pt-Tl-Pt(CN)_5]^{3-}$ (**I**−**V**). The study has revealed that the huge Pt−Tl coupling constants as well as the experimentally observed trend of decreasing J_{Pt-Tl} along the series **I** to **V** is caused by interaction of solvent molecules with the complexes. In particular, the bulk solvent effects have turned out to be surprisingly large, and without consideration of them, not even qualitative agreement with the experimental data can be achieved because the trends are not properly reproduced. Similar effects are found for the $Tl-C^A$ and $Tl-C^B$ coupling constants. All calculated coupling constants in all of the complexes are systematically improved upon introducing more realistic computational models. This suggests a way for future calculations of NMR properties of transition metal complexes. We recommend a model of similar or better quality as our "model C" in order to cover most of the environmental effects as well as to obtain a reasonably good electronic structure. The ZORA method for dealing with the important relativistic effects appears to be well suited for compounds with elements as heavy as Pt and Tl.[50]

At the level of model C, the scalar relativistic calculations are in good agreement with the experimental results obtained from aqueous solution. Remaining sources of errors in the computations are, besides of approximations due to the density functional and the finite basis set, in particular the neglect of spin−orbit coupling (demonstrated in some test calculations to be rather small compared to the solvent effects) and the effects of nuclear vibrations of the solvated clusters. Work along these

(50) Autschbach, J. *Theor. Chem. Acc.*, accepted.

lines is currently pursued. Additionally, the chemical shifts for complexes **I** to **V** have been studied by the present authors. Results will be published elsewhere, demonstrating that also in this case the level of "model C" is required in order to achieve reasonable agreement with experiment.[51]

Spin−spin coupling constants are very sensitive to the geometric and electronic structure as well as environmental effects. Because of the difficulties to calculate these NMR properties accurately, results that differ from experiment by up to 10% can already be regarded as quite satisfactory, in particular, for systems with as many electrons as our present samples. Because of the demonstrated large effects on the coupling constants due to the solvent (complexation, and bulk effects), but also because of the other approximations that have been mentioned above, it perhaps does not make sense to attempt a much better agreement with experiment without simultaneously improving the electronic structure, the geometries, the solvent model, and present approximations in the spin−spin coupling calculations and to include vibrational effects.

We note that from the results of this as well as earlier studies on the NMR properties of transition metal complexes[8−10,20,23] it must be concluded that even qualitative interpretations of NMR spectra, in particular, of spin−spin coupling constants, for such systems might have to consider the presence of solvent molecules for an explanation of the observed trends, signs, and magnitudes. This conclusion is not a priori restricted to heavy metal complexes, though it appears that relativity amplifies the various competing effects.

Acknowledgment. The authors acknowledge financial support from the "Emmy Noether" program of the Deutsche Forschungsgemeinschaft (DFG).

JA0368047

(51) Autschbach, J.; le Guennic, B. *Chem.—Eur. J.*, submitted.